Pakistan Veterinary Journal

ISSN: 0253-8318 (PRINT), 2074-7764 (ONLINE)
Accessible at: www.pvj.com.pk

RESEARCH ARTICLE

Pathological Changes in the Respiratory, Gastrointestinal and Urinary Tracts of Buffalo Calves Following Experimental Hemorrhagic Septicemia

S Annas, MS Abubakar, M Zamri-Saad, FFA Jesse and Z Zunita

Research Centre for Ruminant Diseases, Faculty of Veterinary Medicine, Universiti Putra Malaysia, 43400 Serdang, Malaysia; [1]Department of Veterinary Pathology & Microbiology, Faculty of Veterinary Medicine, Universiti Putra Malaysia, 43400 Serdang, Malaysia
*Corresponding author: mzamri@upm.edu.my

ARTICLE HISTORY (14-035)

Received: January 22, 2014
Revised: April 19, 2014
Accepted: May 31, 2014

Key words:
Gastrointestinal tract
Hemorrhagic septicemia
Respiratory tract
Urinary tract

A B S T R A C T

The present study describes the gross, histopathology and ultrastructural changes in the respiratory, gastrointestinal and urinary tracts of buffalo calves experimentally inoculated with wild-type *Pasteurella multocida* B:2. Six 8-month old buffalo calves were divided into two groups. Calves of Group 1 were inoculated subcutaneously with 5 ml the inoculum containing 10^9 colony-forming unit (cfu)/mL of live wild-type *P. multocida* B:2 while calves of Group 2 were similarly inoculated with 5 ml of sterile phosphate buffered saline. All buffaloes were observed daily for clinical signs before surviving buffaloes were killed on day 3 post-inoculation for gross and histology examinations of the respiratory, gastrointestinal and urinary tracts. All infected calves of Group 1 were dead between 6 and 12 h post-inoculation with typical gross lesions of hemorrhagic septicemia. The respiratory, gastrointestinal and urinary tracts showed moderate to severe congestion and hemorrhages. Frothy fluid and fibrin were found in the respiratory tract while the content of gastrointestinal tract appeared soft, watery and occasionally blood-tinged. The urinary tract contained blood-tinged urine. Histologically, the organs of respiratory, gastrointestinal and urinary tracts showed varying degrees of congestion and hemorrhages with endothelial destruction. The right middle lung lobe, the small intestines and kidneys showed significantly more severe histological lesions. Ultrastructure examination revealed the presence of *P. multocida* B:2 on the erythrocytes and the endothelium of the respiratory, gastrointestinal and urinary tracts. Similarly, *P. multocida* B:2 was successfully isolated from all samples collected from these tracts, suggesting the involvement of these body systems in transmission of the disease.

To Cite This Article: Annas S, MS Abubakar, M Zamri-Saad, FFA Jesse and Z Zunita, 2015. Pathological changes in the respiratory, gastrointestinal and urinary tracts of buffalo calves following experimental hemorrhagic septicemia. Pak Vet J, 35(4): 430-435.

INTRODUCTION

Pasteurella multocida B:2 (Asian serotype) and E:2 (African serotype) are known to cause hemorrhagic septicemia (HS) of cattle and buffaloes (Ahmed, 1996; Rafidah *et al.*, 2010). It is a highly fatal disease with a short clinical course (Khan *et al*., 2011). Infection is generally believed to establish via the respiratory route, which eventually leads to septicemia and acute death (Benkirane and De Alwis, 2002; Mitra *et al.*, 2013).

Recently, the involvement of oral route in HS infection has been re-emphasized following isolation of *P. multocida* B:2 from the organs of gastrointestinal tract (Abubakar and Zamri-Saad, 2011; Abubakar *et al*., 2013). Although the detailed pathological changes in the respiratory tract have been described, pathological changes in the gastrointestinal and urinary tracts have not been well documented, and the pathogenesis is not fully understood. This report describes and evaluates the gross, histological and ultrastructural changes in the respiratory, gastrointestinal and urinary tracts of buffalo calves experimentally infected with *P. multocida* B:2.

MATERIALS AND METHODS

Animals: Six 8-month old clinically healthy buffalo calves *(Bubalus bubalis)* from a farm with no history of outbreak and vaccination against HS were selected. The

calves were acclimatized for a period of 5 days and were treated with anthelmintic. They were ensured to be free from *P. multocida* for two weeks prior to the start of the experiment by isolation from nasal swabs (Zamri-Saad *et al.*, 2006). Blood sera were collected and subjected to enzyme-linked immunosorbent assay (ELISA) to ensure that the calves had low specific antibody titer (Zamri-Saad *et al*., 2006). The calves were fed cut grass and supplemented with palm kernel-based pellets at the rate of 400 g/calf/day. Drinking water was available *ad libitum*. Access to veterinary care was available at all times and the well being of the calves was assessed regularly.

***Pasteurella multocida* B:2:** Stock culture of *P. multocida* serotype B:2 isolated from an outbreak of HS was re-confirmed before used (Rajeev *et al.*, 2011). The organism was cultured onto blood agar at 37°C for 24 h. Four colonies of the organism were then seeded into brain-heart infusion (BHI) broth and incubated at 37°C with shaking at 150 rpm for 18 h. Serial dilution method was used to determine the bacterial concentration in the BHI broth and sterile phosphate buffered saline was used to dilute the inoculum to a final concentration of $1.0x10^9$ colony forming unit (cfu/mL of *P. multocida* B:2 (Rafidah *et al.*, 2012).

Experimental design: The calves were divided equally into two groups and were kept in separate house. In each house, the calves were kept in individual pen. At the start of the experiment, all calves of Group 1 were challenged subcutaneously at the shoulder region with 5 ml of the inoculums containing $1.0x10^9$ cfu/ml of live wild-type *P. multocida*B:2 (Annas *et al.*, 2014). Calves of Group 2 were similarly inoculated with 5 ml of sterile phosphate buffered saline. After inoculation, all calves were observed daily for clinical signs of HS. When the calves showed high fever and recumbent, they were killed according to the guideline of the Ethics Committee, Universiti Putra Malaysia. Surviving calves were killed at the end of day 3 post-inoculation. All experimental protocols were approved the Ethics Committee, Universiti Putra Malaysia.

Gross lesion evaluations: Necropsy was conducted immediately after death. At necropsy, attention was focused on the respiratory, gastrointestinal and urinary tracts. Gross lesions were scored according to the method described earlier (Abubakar and Zamri-Saad, 2011) following visual examination and palpation. Briefly, no significant lesions were scored 0, 5-10% surface affected was scored 1, 11-25% scored 2 and over 25% scored 3.

Histopathological evaluations: Samples of the lungs, liver, rumen, reticulum, omasum, abomasum, duodenum, jejunum, ileum, caecum, colon, rectum, kidney and urinary bladder were immediately fixed in 10% neutral buffered formalin for at least 12 h. The samples were processed routinely for histopathological examination using the paraffin embedded technique, sectioned at 4 µm and stained with hematoxylin and eosin. The histological sections were viewed at five random fields at high power and the lesions were scored based on severity according to a method described previously (no significant lesion = 0, mild lesion = 1, moderate lesion = 2, and severe lesion = 3) (Abubakar and Zamri-Saad, 2011).

Ultrastructural evaluations: The same organ samples were trimmed into $1mm^3$ before they were fixed in 4% glutaraldehyde in 0.1 M sodium cacodylate buffer for 18 h at 4°C. The samples were routinely processed for TEM according to Cheville (2009). Samples were trimmed and sectioned using ultra-microtome (Leica, EM KMR 2UTC, Germany) at 80 nm thick, placed onto copper grids and stained with 5% uranyl acetate and lead citrate. All the samples were examined and photographed under transmission electron microscope (Leo 912 AB EFTEM, Omega Filtering system, Germany). Viewing was done at nine random positions across the sections. The ultrastructural changes were described and scored based on the characteristics of response to cellular injury (Abubakar *et al.*, 2013) with modification from the method previously described (Paul *et al.*, 1995). The response to cellular injury was considered as mild if predominant changes were of early events and scored 1, moderate when predominant changes were of intermediate events and scored 2, while changes considered severe were scored 3. Score 0 was given if the section was normal.

Statistical analysis: Data were analyzed using one-way ANOVA to compare the severity in different segments of the respiratory, gastrointestinal and urinary tracts. Data were expressed as mean±SD of severity. All statistical analyses were done using SPSS version 21.

RESULTS

Clinical response and bacterial isolations: Following subcutaneous inoculation, all infected calves of Group 1 had to be killed between 6 and 12 h post-inoculation following advanced clinical signs. The first calf was killed at 6 hours, another at 10 h and the third at 12 h post-inoculation. All affected calves of Group 1 appeared depressed and dull, recumbent, anorexic, pyrexic, dyspneic with profused nasal discharge and had diarrhea. *Pasteurella multocida* B:2 was successfully isolated from all organ samples, including the rectal, nasal and urinary bladder swabs, and the urine sample. All calves of Group 2 survived the experiment and were killed on day three post-inoculation.

Gross lesions: Grossly, all calves of Group 1 showed similar gross changes typical of HS, which included severe congestion and hemorrhages at the mucosal surfaces of all tracts, the subcutaneous tissues and in most organs of the respiratory, gastrointestinal and urinary tracts. There was presence of fibrin on the serosal surfaces of all thoracic and abdominal organs.

The respiratory tract showed severe congestion and multifocal ecchymotic hemorrhages of the larynx, trachea and the lungs (Fig. 1A) with presence of frothy fluid within the trachea, bronchi and bronchioles. Fibrin deposition was noted on the surface of the lungs (Fig. 1B). Approximately 150 ml of blood-tinged fluid accumulated in the thoracic and abdominal cavities. The gastrointestinal tract showed moderate congestion and mild multifocal ecchymotic hemorrhages on the serosal

surface, with diffuse fibrin deposits (Fig. 1C, D). Mucosal surface of the abomasum showed severe congestion with ecchymotic hemorrhages but the rumen, reticulum and omasum showed mild, focal congestion. Similarly, the small and large intestines showed ecchymotic and paint brush hemorrhages, congestion and thickened wall (Fig. 1E,F). The kidneys showed severe congestion while the urinary bladders showed mild to moderate congestion with multifocal paintbrush hemorrhages, containing blood-tinged urine. No gross lesions were observed in buffalo calves of the negative control Group 2.

Severity of gross lesions: The respiratory tract was found to show significantly ($P<0.05$) more severe gross lesions than the gastrointestinal and urinary tracts (Table 1). Within the gastrointestinal and urinary tracts, the abomasum and kidney showed significantly ($P<0.05$) higher lesion score. No significant ($P>0.05$) difference was noted between the severity of lesions among the other organs of the small and large intestines. The forestomach, particularly the rumen and reticulum were found to show significantly ($P<0.05$) lowest gross lesions score.

Histopathology: All infected calves of Group 1 showed similar histopathological changes. The lungs were severely congested with multifocal hemorrhages within the alveolar spaces (Fig. 2A). Bacterial colonies were observed within the alveolar spaces, the lumen of bronchioles (Fig. 2B) and some capillaries. All major blood vessels were congested while the bronchioles were filled with fibrin, edema fluid, necrotic cells and desquamated bronchiolar epithelial cells.

Most hepatocytes were swollen with eosinophilic cytoplasm while some hepatocytes showed pyknotic nuclei. Blood vessels and the sinusoids were congested. Circulating neutrophils and macrophages were seen in the lumen of some hepatic blood vessels. Mild multifocal hemorrhages were found distributed within the entire sections of the liver.

Examination of the rumen, reticulum and omasum revealed few inflammatory cell infiltrations in between the epithelial cells. The subepithelial space and submucosal connective tissue were loosely arranged due to edema. There were occasional multifocal hemorrhage, bacterial colonies and fibrin. Similarly, the spaces between muscle bundles were expanded with bacterial colonies. Some endothelia were desquamated leading to moderate multifocal hemorrhages.

The abomasum showed moderate to severe congestion with moderate to severe macrophage and neutrophilic infiltrations in between the epithelial cells (Fig. 2C). The submucosa layer was edematous and severely hemorrhagic. Bacterial colonies were noted in abundance within the submucosa and muscularis layers of the abomasums. Endothelial desquamation was occasionally observed.

The mucosal layer of duodenum and jejunum were diffusely infiltrated by macrophages and neutrophils. There was moderate desquamation of the cells lining the crypts of Lieberkhun with multifocal hemorrhages in all layers of the duodenum, most severely in the mucosal layer. Complete loss of normal architecture and cellular structures was observed at the tip of the villi. The blood vessels were severely congested while some showed desquamation of the endothelium.

The mucosal layer of ileum had focal ulcerations with necrosis of the villi and the glandular cells. There was depletion of the Payer's patches leaving empty spaces filled with bacterial colonies. All blood vessels surrounding the affected Payer's patches were severely congested with moderate hemorrhages. Similarly, the caecum, colon and rectum had mild to severe erosions with multifocal moderate infiltration of neutrophils and macrophages (Fig. 2D).

The kidneys showed moderate to severe multifocal tubular necrosis and hydropic degeneration of the epithelium (Fig. 2E). The renal blood vessels were congested with few monocytes. Cast depositions were observed in the lumen of most renal tubules and in the widened Bowman's capsules following glomerular atrophy. Connective tissue of the urinary bladder was severely edematous with bacterial colonies in between the muscle bundles. Erythrocytes were observed in the lumen as well as in the wall of urinary bladder (Fig. 2F). No histology lesion was found in the control uninfected buffalo calves of Group 2.

Severity of histopathology lesions: The respiratory tract had significantly ($P<0.05$) highest overall histopathology lesion score (Table 1). All lobes of the lungs had significantly ($P<0.05$) higher lesion scores than the rumen, reticulum, omasum and urinary bladder. Significantly ($P<0.05$) highest lesion score was recorded for the right middle lung lobe of the respiratory tract, the small intestinal segments of the gastrointestinal tract, and the kidney of the urinary tract while significantly ($P<0.05$) lowest lesion score was recorded for the fore-stomachs.

Ultrastructural changes: There were numerous short rod bacterial cells of 1-2.3µm length and 0.2-0.4µm width surrounded by halo space suggestive of *P. multocida* B:2 both intra and extravascular. The bacteria were observed within blood vessels of most organs in close association with the erythrocytes and endothelial cells. The bacteria were also observed inside some lysed endothelial cells. In sections where endothelial damage was severe, the bacteria were observed to invade the tissues from the capillaries.

The pneumocytes showed extensive disintegration of nuclear envelope, peripheral nuclear condensation, severe nuclear invagination and nuclear membrane fragmentation and blabbing. Some capillaries of the lungs were devoid of endothelial cells, leaving the basement membrane exposed and lost its continuity while others had degenerated and necrotic endothelial cells. Ballooning of mitochondria with partial to complete cristolyis were frequently observed, while fragmentation of cytocavitary network membranes was occasionally observed in few samples. Large numbers of bacteria were observed in and around the blood vessels.

The hepatocytes showed marked peripheral nuclear condensation due to nucleoplasmic rarefaction and nuclear membrane fragmentation. There were cytoplasmic edema, mitochondrial swelling, cristolysis and matrix lysis. Some hepatocytes had undergone lysis with presence of bacteria in the cytoplasm. The bacteria were also observed in close association with the erythrocytes, leading to depression on the surface of the affected

erythrocytes (Fig. 3A). *Pasteurella multocida* B:2 was observed only in the abomasum, mostly within the lysed endothelial cells (Fig. 3B).

There was cytoplasmic edema of the endothelial and epithelial cells of the duodenum, jejunum, and ileum. Mitochondrial swelling and cristolysis were present, while *P. multocida* B:2 was observed only in the duodenum and ileum. Complete lysis of the endothelial cells surrounding the affected capillaries was observed. Polymorphonuclear inflammatory cells with irregular nuclear membranes were observed in all three organs and the cecum. The colon and rectum showed severe endothelial and epithelial nucleoplasm rarefaction, nuclear envelope collapse and invaginated. Many bacterial cells were observed both intra and extravascularly (Fig. 3C).

Bacteria suggestive of *P. multocida* B:2 was found attached to the basement membrane of capillaries, and within the cytoplasm of lysed tubular epithelium of kidneys (Fig. 3D). Affected cells showed evidence of peripheral chromatin condensation, severe nuclear envelope disintegration and complete lysis and destruction of tubular cells. The bacteria were also found in close association with the erythrocytes and within the lumen of urinary bladder.

The ultrastructural examination of control uninfected buffalo calves of Group 2 revealed no ultrastructural changes.

Severity of ultrastructural changes: Significantly highest ($P<0.05$) ultrastructural lesion score was recorded in the lungs. Within the gastrointestinal tract, the abomasum showed significantly ($P<0.05$) highest ultrastructural lesion score. Within the urinary tract, the kidneys were observed to have the highest ($P<0.05$) lesion score (Table 1).

DISCUSSION

The present study reports for the first time, the histopathological and ultrastructural changes in the respiratory, gastrointestinal and urinary tracts of buffalo calves following peracute HS. The severities of gross, histopathological and ultrastructural lesions were compared between and within the body systems. All infected animals exhibited classical clinical signs of HS, which are in agreement with previously described in both natural (Khan *et al.,* 2011) and experimental infections involving goats, cattle and buffaloes (Zamri-Saad and Shafarin, 2007; Khin *et al.,* 2010; Abubakar and Zamri-Saad, 2011). The gross, histopathological and ultrastructural lesions described in the present study were similar to those described earlier in experimental HS (Shafarin *et al.,* 2009; Abubakar and Zamri-Saad, 2011; Abubakar *et al.,* 2013) but with different degree of severity. Furthermore, the present study describes peracute lesions and ultrastructural interactions of the bacteria with the endothelial cells in the respiratory, gastrointestinal and urinary tracts. The varying degrees of the severity were largely dependent on the route of infection (Zamri-Saad and Shafarin, 2007), age of the animal and the dosage of infection.

Based on the lesion severity score, the lungs remained as the most important and the most severely affected organ. However, the abomasum, small intestine and kidney showed consistently high lesion scores. Furthermore, *P. multocida* B:2 was successfully isolated from the rectal and urinary bladder swabs as well as from the urine, which re-emphasized the possible transmission of *P. multocida* B:2 through these systems, as previously suggested (De Alwis, 1992; Abubakar and Zamri-Saad, 2011).

Ultrastructural examinations revealed the detailed *in vivo* interaction between *P. multocida* B:2 and the host. Although the ultrastructural lesions were similar as previously described (Abubakar *et al.*, 2013), the present study revealed much severe changes resulting from peracute cellular response (Zamri-Saad and Shafarin, 2007). Similarly, this study revealed large numbers of bacteria suggestive of *P. multocida* B:2 in most samples, possibly due to the fact that the calves succumbed to the disease at the peak of the septicemic stage. Furthermore, invasion or translocation through endothelial cells is necessary for rapid invasion of the vascular system for successful septicemic disease (Galdiero *et al*., 2001).

Table 1: Gross, histopathological and ultrastructural lesions scoring (Mean±SD) for the respiratory, gastrointestinal and urinary tracts following experimental exposure to *P. multocida* B:2

System	Location	Severity Score of Lesions		
		Gross	Histopathological	Ultrastructural
Respiratory	Right cranial cranial	3.00 ± 0.00^{a}	2.47 ± 0.44^{a}	2.89 ± 0.33^{a}
	Right cranial caudal	(Lungs)	2.50 ± 0.53^{a}	(Lungs)
	Right middle		2.70 ± 0.52^{a}	
	Right caudal		$2.37\pm0.44^{a,b}$	
	Left cranial		2.47 ± 0.55^{a}	
	Left middle		2.47 ± 0.35^{a}	
	Left caudal		2.47 ± 0.58^{a}	
	Accessory		2.43 ± 0.46^{a}	
Gastrointestinal	Liver	$2.33\pm0.58^{a,b,c}$	$2.07\pm0.63^{a,b}$	$2.00\pm1.12^{a,b,c,d}$
	Rumen	0.33 ± 0.58^{c}	1.13 ± 0.81^{c}	0.56 ± 0.53^{e}
	Reticulum	0.33 ± 0.58^{c}	0.90 ± 0.60^{c}	$0.89\pm0.78^{d,e}$
	Omasum	$0.67\pm0.58^{b,c}$	0.90 ± 0.74^{c}	0.78 ± 0.83^{e}
	Abomasum	$2.67\pm0.58^{a,b}$	$2.03\pm0.88^{b,c}$	$2.67\pm0.50^{a,b}$
	Duodenum	$2.33\pm1.15^{a,b,c}$	2.50 ± 0.60^{a}	$2.33\pm0.50^{a,b,c}$
	Jejunum	$1.33\pm0.58^{a,b,c}$	2.43 ± 0.56^{a}	$2.33\pm0.71^{a,b,c}$
	Ileum	$2.00\pm1.00^{a,b,c}$	2.43 ± 0.56^{a}	$2.33\pm0.71^{a,b,c}$
	Cecum	$1.67\pm0.58^{a,b,c}$	$2.27\pm0.56^{a,b}$	$2.11\pm1.05^{a,b,c}$
	Colon	$1.67\pm1.15^{a,b,c}$	$2.23\pm0.73^{a,b}$	$1.33\pm0.71^{c,d,e}$
	Rectum	$1.67\pm0.58^{a,b,c}$	$2.17\pm0.59^{a,b}$	$2.22\pm0.83^{a,b,c}$
Urinary	Kidney	$2.67\pm0.58^{a,b}$	2.67 ± 0.37^{a}	$2.56\pm0.53^{a,b}$
	Urinary Bladder	$1.33\pm0.58^{a,b,c}$	1.00 ± 0.76^{c}	$1.67\pm0.71^{b,c,d,e}$

Different superscripts within the same column indicate significant difference ($P<0.05$).

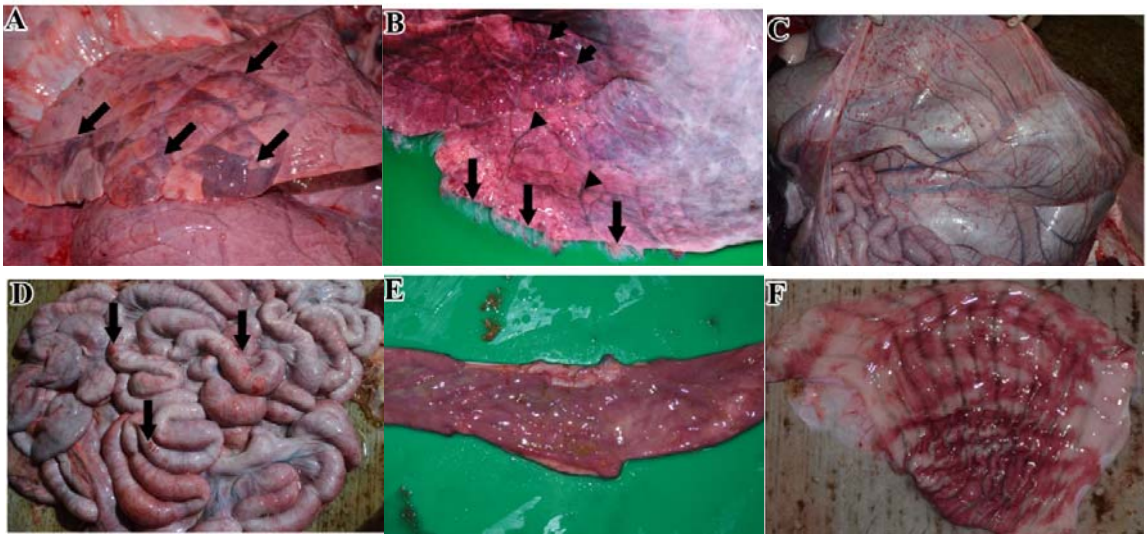

Fig. 1: (A) Areas of acute pneumonia (arrows) in the lung parenchyma. (B) Severe congestion of the lungs with fibrin on the edges (long arrows), atelectasis (short arrows) and inter-lobular edema (arrowheads). (C) Presence of fibrin on the omentum. (D) Congestion and petechiation (arrows) at the serosal surface of the gastrointestinal tract. (E) Severe congestion and thickening of duodenal mucosal surface. (F) Diffuse paint brush hemorrhages at the mucosal surface of the colon.

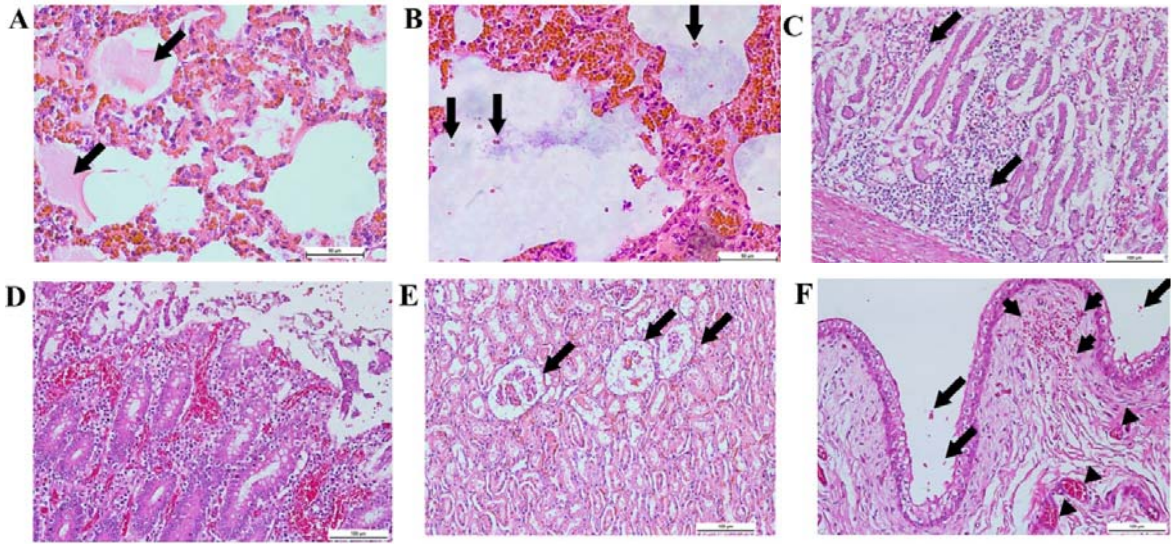

Fig. 2: (A) Congested lungs with edema fluid (arrows) (HE, bar=50 µm). (B) Severe congestion and mild hemorrhages (arrow) in the lungs with bacterial colonies (basophilic staining) in the alveolar space (HE, bar=50 µm). (C) Focal infiltration of neutrophils and macrophages (arrows) in the mucosal layer of the abomasum (H, bar=100 µm). (D) Severely congested blood vessels, diffuse infiltration of inflammatory cells, hemorrhage and erosion of the rectal mucosa (HE, bar=100 µm). (E) Hydropic degeneration of tubular epithelium with atrophied renal corpuscles (arrows) (H, bar=100 µm). (F) Free RBC in the lumen of urinary bladder (long arrows) and in subepithelial layer (short arrows). Blood vessels are congested (arrowheads) (HE, bar=100 µm).

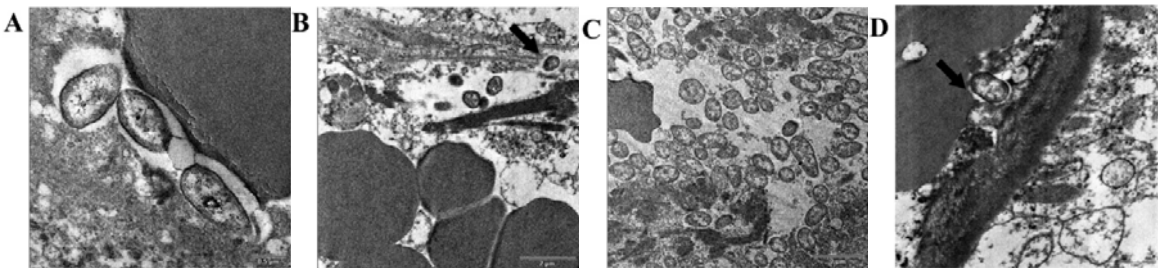

Fig. 3: (A) Close attachment of bacterial cells to the cell membrane of RBC within liver (TEM, bar=0.5 µm). (B) Presence of bacteria in a lysed endothelial cell of abomasum. Note a bacterium is translocating across the damaged endothelium (arrow) (TEM, bar=2 µm). (C) Ruptured and severely damaged capillary of colon with numerous bacteria cells (TEM, bar=2 µm). (D) A bacterium was found attached to the basement membrane of a capillary in kidney (arrow). (TEM, bar=1 µm).

In most organs, the bacteria were observed to attach to the cytoplasmic membrane of red blood cells (RBC), suggesting high affinity of *P. multocida* B:2 towards RBC. Attachments of the bacteria onto the intact, injured or lysed endothelial cells and its basement membrane were also frequently observed. An important stage in the pathogenesis of infections by *P. multocida*B:2 is the translocation through epithelial tissues to reach the vascular system (Dugal *et al*., 1992; Lee *et al*., 1994). The potential to adhere to and invade cells by translocation may constitute a mechanism which enables the bacteria to invade the bloodstream. In the present experiment, it was observed that the endothelial cells and their basement membranes were severely affected. From the lumen of blood vessels, the agent and its endotoxin exert damaging effects to the endothelial cells and their basement membrane, thus eventually leads to lysis of the endothelium. Damages to the endothelial cells affect the balance of fluid in the interstitial tissues, leading to escape of cells, fluid and proteinous materials from the vascular system. This triggers other events including hemorrhages, edema and congestion (Breider *et al*., 1990). *Pasteurella multocida* B:2 has been described to live in intact endothelium (Galdiero *et al*., 2001), however, the present study observed the agent in the cytoplasm of lysed endothelial cells. The study confirmed the involvement of the respiratory tract as the most pathologically affected system in peracute HS, and suggests the importance of some parts of the gastrointestinal and urinary tracts in the development and transmission of HS. The present study revealed the close interaction of *P. multocida* B:2 with the RBC and the endothelial cells, which is valuable in suggesting another mechanism of invasion of *P. multocida* B:2 from the blood stream into the organ parenchyma and vice versa.

Acknowledgment: The ERGF Grant from the Ministry of Higher Education, Malaysia, assisted this study financially.

REFERENCES

Abubakar MS and M Zamri-Saad, 2011. Clinico-pathological changes in buffalo calves following oral exposure to *Pasteurella multocida* B:2. Basic Appl Pathol, 4: 130-135.

Abubakar MS, M Zamri-Saad and S Jasni, 2013. Ultrastructural changes and bacterial localization in buffalo calves following oral exposure to *Pasteurella multocida* B: 2. Pak Vet J, 33: 101-106.

Ahmed S, 1996. Status of some bacterial diseases of animals in Bangladesh. Asian Livest, 21: 112-114.

Annas S, M Zamri-Saad, FFA Jesse and Z Zunita, 2014. New sites of localization of *Pasteurella multocida* B:2 in buffalo surviving experimental hemorrhagic septicemia. BMC Vet Res, 10: 88

Benkirane A and MCL De Alwis, 2002. Hemorrhagic septicemia, its significance, prevention and control in Asia. Vet Med-Praha, 47: 234-240.

Breider MA, S Kumar and RE Corstvet, 1990. Bovine pulmonary endothelial cell damage mediated by *Pasteurella haemolytica* pathogenic factors. Infect Immun, 58: 1671-1677.

De Alwis MCL, 1992. Haemorrhagic septicaemia: a general review. Brit Vet J, 148: 99-112.

Dugal F, M Belanger and M Jacques, 1992. Enhanced adherence of *Pasteurella multocida* to porcine tracheal rings preinfected with *Bordetella bronchiseptica*. Can J Vet Res, 56: 260-264.

Galdiero M, L De Martino, U Pagnini, MG Pisciotta and E Galdiero, 2001. Interactions between bovine endothelial cells and *Pasteurella multocida*: association and invasion. Res Microbiol, 152: 57-65.

Khan A, MK Saleemi, MZ Khan, ST Gul, M Irfan *et al*., 2011. Hemorrhagic septicemia in buffalo (*Bubalus bubalis*) calves under sub-tropical conditions in Pakistan. Pak J Zool, 43: 295-302.

Khin MN and M Zamri-Saad, 2010. The effect of dexamethasone on immune responses of calves to intranasal exposures to live attenuated gdhA derivative of *Pasteurella multocida* B:2. Pertanika J Trop Agric Sci, 33: 205-211.

Lee MD, R Wooley and JR Glisson, 1994. Invasion of epithelial cell monolayers by turkey strains of *Pasteurella multocida*. Avian Dis, 38: 72-77.

Mitra J, M Chowdhury and C Bhattacharya, 2013. Outbreak of jemorrhagic septicemia in free range buffalo and cattle grazing at riverside grassland in Murshiabad district, West Bengal, India. J Expl Anim Med Res, 3: 178-182

Paul SM, LP Nguyen and HV Vinters, 1995. Cerebral cortical dysplasia associated with pediatric epilepsy. J Neuropath Exp Neur, 54: 137-153.

Rafidah O, M Zamri-Saad, E Nasip, S Shahirudin and AA Saharee, 2010. Analysis of hemorrhagic septicaemia outbreaks in cattle and buffalo in Malaysia. Online J Vet Res, 14: 325-333

Rafidah O, M Zamri-Saad, S Shahirudin and E Nasip, 2012. Efficacy of intranasal vaccination of field buffaloes against haemorrhagic septicaemia with a live *gdhA* derivative *Pasteurella multocida* B:2. Vet Rec, 171: 175

Rajeev R, SK Panda, AP Acharya, AP Singh and MK Gupta, 2011. Molecular diagnosis of hemorrhagic septicemia - a review. Vet World, 4: 189-192

Shafarin MS, M Zamri-Saad, B Siti Khairani and AA Saharee, 2009. Pathological changes in the respiratory tract of goats infected by *Pasteurella multocida* B:2. J Comp Pathol, 140: 194-197.

Zamri-Saad M, ZA Ernie and MY Sabri, 2006. Protective effect following intranasal exposure of goats to live *Pasteurella multocida* B:2. Trop Anim Health Pro, 38: 541-546.

Zamri-Saad M and MS Shafarin, 2007. Response of goats to the different routes of infection by *Pasteurella multocida* B:2. J Anim Vet Adv, 6: 340-343.